Factorial Optimization of the Effects of Melt-Spinning Conditions on Biodegradable As-Spun Aliphatic–Aromatic Copolyester Fibers. III. Diameter, Tensile Properties, and Thermal Shrinkage

Basel Younes,[1,2] Alex Fotheringham[1]

[1]*School of Textiles and Design, Heriot-Watt University, Scottish Borders Campus, Netherdale, Galashiels TD1 3HF, United Kingdom*
[2]*Faculty of Mechanical and Electrical Engineering -Textiles Dep., Damascus University, Damascus, PO.BOX 86, Syria*

Received 22 November 2010; accepted 25 January 2011
DOI 10.1002/app.34216
Published online 23 May 2011 in Wiley Online Library (wileyonlinelibrary.com).

ABSTRACT: To model the melt-spinning process of biodegradable as-spun linear aliphatic–aromatic copolyester fibers, a fraction factorial experimental design and appropriate statistical analysis for the 32 screening trials involving five control parameters were used. Because of their central role in the production processes and end use textiles, it is important to simulate the mechanical and thermal shrinkage properties of AAC fibers. Concise statistical models of fiber behavior are based on factorial experimental design data. Process's data are collected, analyzed, and mathematical models created to predict the diameter, tenacity, elongation at break, modulus, and thermal shrinkage of the spun fiber in terms of random variables and their associated probability distributions. The theoretical regression models obtained form the main source code in the enhanced forecasting program, which presents the melt-spinning process of aromatic–aliphatic copolyester fibers. Factorial statistical approaches, based on over indicated region levels of melt-spinning process parameters, are given in terms of assumptions and theory to produce biodegradable, environmentally friendly fibers for different applications. © 2011 Wiley Periodicals, Inc. J Appl Polym Sci 122: 1434–1449, 2011

Key words: modeling; biodegradable; aliphatic–aromatic copolyester fibers; factorial experimental design; mechanical and thermal properties

INTRODUCTION

Previously, researchers' work has been conducted to improve and characterize biodegradable aliphatic–aromatic copolyesters.[1–10] Aliphatic–aromatic copolyesters (AACs) are made from petroleum with stable physical and chemical properties while leaving no environmental footprint.[11] In an active microbial environment, the copolyesters' products become invisible to the naked eye within 12 weeks.[12] AACs are potential candidates to make fibers for various nonwoven materials particularly for expendable uses in medicine[13–15] and agriculture.[16–20]

As it is difficult to design and produce a manufactured product, the experimental design technique is a useful practice for designing new, consistent, and economical products.[21] Measurement, feedback and adjustment, prediction, and correction are the main elements in online quality control.[22,23] Practical software-based approaches meet with customer requirements and expectations for reducing the target value variation in processes[24–26] and saving time and cost.[27] Statistical experimental design (SED) is still limited because of poor attitude toward the SED strategies and lack of collaboration between academic and industrial fraternities.[28]

As spun fibers should have a structure that can be drawn easily, the stress–strain behavior can also be used to qualitatively describe and classify the polymer and its fibers properties and behavior. The % of fiber extension could be limited by crosslinking of the polymer structure, which will affect the biodegradability of the fibers.[29] As the continuous filament yarn has the same number of fibers in the cross section, physicomechanical properties will be influenced uniformly by constant stretching the fibers through or after spinning[30]; a high degree of extension gives higher tenacity together with lower elongation at break (high modulus) and vice versa.[31] The increased modulus and tensile strength could be related to the increasing of down draw ratio. A balance between the improvement of mechanical properties and the biodegradability needs to be investigated.[32]

Textile fibers with thermoplastic properties have created the need for the testing of thermal shrinkage or extension of yarns and fabrics made from such materials when subjected to heat. Many important physical properties are affected when fibers are set.

Correspondence to: A. Fotheringham (a.f.fotheringham@hw.ac.uk).

Thermal properties are important if the fibers undergo heat treatment during processing as well as in use. With increasing mobilization of chains, the thermodynamically beneficial random coil state is approached, and heat causes a softening of the noncrystalline region.[33] Some unstability can be obtained when the fibers are heated to practical application temperatures such as washing and ironing processes.[34] In setting mechanism and by recrystallization: fibers are deformed, the internal stresses are relaxed, and the new form is stabilized.[35]

In this article, different samples of linear as-spun AAC fibers were spun at different process parameters to determine and model their effects. The target was to demonstrate how variation in spinning conditions can affect the diameter, tensile properties, and thermal shrinkage, which will give a better insight into the relationship between melt-spinning process parameters and produced fiber properties. The theoretical regression models obtained form the main source code in the enhanced forecasting program, which presents the melt-spinning process of aromatic–aliphatic copolyester fibers.

EXPERIMENTAL

Material

A fully biodegradable, petroleum, aromatic–aliphatic copolyester (solanyl flexibility component), based on butandiol, adipic acid, and terephthalic acid, was supplied by Rodenburg Company, Netherlands, and used in this work. The polymer shape is spherical granule resin in diameter 3–5 mm, with density of 1.2 g/cm^3. The range of melting temperatures T_m is 110–115°C. The material is referred to[36]: 1,4-benzenedicarboxylic acid, polymer with 1,4-butanediol, and hexanedioic acid. Because of the low water solubility and high molecular weight of the polymer, it is unlikely to bioaccumulate.[37] No ecotoxicity data were submitted,[38] and no significant toxicological effect was observed.[39] Because the effective glass transition temperature T_g is below the normal operation temperature (around −30°C), the crystallization will go to equilibrium very slowly. To solve this problem, it is necessary to heat the extruded polymer in an inert atmosphere at some temperature between T_g and T_m, which will stabilize the polymer as a practice used in similar processes.[40] The polymer was dried at 60°C for 6 h before use to avoid possible hydrolysis during the extrusion process. Grade AAC1 was selected based on the results achieved in previous work.[41–44]

Fiber diameter

The characterization of fibers' diameter was carried out using a Leitz Diaplan optical microscope connected to Digital Olympus ALTRA 20 camera with Olympus Imaging Software. Fiber samples were selected randomly and put onto a microscope yarn holder. The fiber diameter was measured in five various axial positions for 10 individual fibers selected, and the mean values and deviations of diameter were calculated.

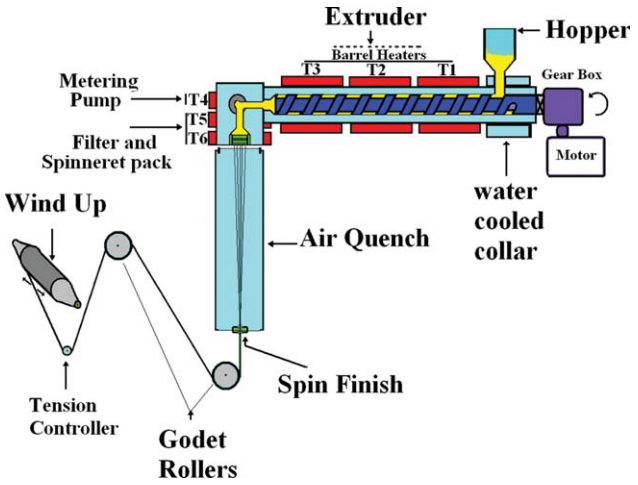

Figure 1 Schematic diagram of the melt-spinning equipment. [Color figure can be viewed in the online issue, which is available at wileyonlinelibrary.com.]

Melt spinning

Fibers were extruded via melt spinning on a Lab-Spin machine, Extrusion Systems Limited, UK. The Lab-Spin machine (Fig. 1) consists of a single-screw extruder barrel (25 mm screw with length/diameter ratio 20 : 1), a metering pump, a die head, an air cooling window, a spin finish application system, and a winding system. Aliphatic–aromatic copolyester granules are fed through the hopper into the extruder, then mechanically compressed, and melted. The molten polymer is forced through a special designed spinneret, which has 30 holes (0.4 mm diameter, l/day = 2) as fine jets with speed adjusted by the metering pump. The filaments were then cooled down and harden through the air cooling quench at room temperature progressively to emerge as solid filaments. The spin finish oil, VICKERS 1031, was diluted fivefold with water before use. The six heaters in the extrusion machine are electrically heated, and the temperatures were controlled independently by thermocouples. The energy required to melt the polymer comes from both external heating and the internal friction.[25] The godets and the winder speed are controlled independently by DC motors. The tension in the Leesona winder is controlled automatically to have good package build up and to avoid the high tension that affect on the filament properties, and all the speeds were

investigated by laser digital tachometer. The temperature of feeding zone should be above 100°C to prevent any moisture from forming.

Characterization of mechanical properties

Tensile testing of fibers was carried out using a tensile tester (Instron 3345) at a temperature of (20 ± 2)°C and relative humidity of 65% ± 5%. Linear density (denier) was determined by weighing a 100-m length by using a balance accurate to 1 mg. Specimens were cut from the continuous filaments with 2 cm length to be used in the mechanical tests. The samples were conditioned at a temperature of (20 ± 2)°C and relative humidity of 65% ± 5% for 48 h before testing. The initial gauge length 20 mm was stretched at a constant cross-head speed 200 mm/min for each sample. The reported results were the average values of five repeated measurements. Through testing the material until break, it has been determined that the filament passes through many regions including elastic region, yielding, strain hardening, necking, and failure. The elongation at break was measured as a percentage of the original length.[45,46] Some filaments deform in the thin section by elongation at break as load is increased. At the yield point, the tensile filament starts to neck down and continues necking till the sample ruptures in the elastic region.[47]

Factorial experimental design

Experimental design gives information about the significance of the main effect factors and their interactions and then provides further information on how to optimize the average response values depending on the factor levels. First, some pre-experimental work must be done to determine the number and the levels of factors and to prepare the matrix design and the number of trials. After this process, a fraction factorial experimental design (L32) with random order is used[48,49] for the 32 screening trials involving five control parameters and two levels for each parameter. The five control parameters for the melt spinning are metering pump speed (MPS), melt extrusion (or melt-spinning) temperature (T), quenching air speed (QA), applied speed of spin finish (SF), and winding speed (WS). The two levels of each parameter were separated as far apart as possible from one another as shown in Table I. The experiments were conducted in one block. The model was limited only to two-parameter interactions, because interactions of more than two parameters are not useful in practice. The matrix design, statistical analysis, and presented analysis plots are constructed directly from the raw data using MINITAB and STATGRAPHICS programs. Samples' data are analyzed, and the significant factors are determined to develop the process design.[50] Because the unsuspected factor's change with time may distort the analysis and result in misleading conclusions,[51] randomly errors could be separately distributed. There are many tools used in the statistical analysis of experimental design such as the Pareto chart, the effect plot, normal probability plot, surface plot, interaction plot, and analysis of variance (ANOVA). The theoretical basics about these tools will be described later.

TABLE I
Factors and Their Levels for the Spinning Experiment

Factor's abbreviation	Factor name	↓ Level	↑ Level
T	Melt extrusion (spinning) temperature (°C)	130	145
MPS	Metering pump speed (rpm)	6	12
QA	Quench air speed (%)	35	50
SF	Spin finish speed (rpm)	0.35	0.50
WS	Winding speed (m min^{-1})	50	100

Scanning electron microscope

Using a Polaron THERMO VG SCIENTIFIC SC 7620—scanning electron microscopy (SEM) Sputter Coater, the samples were coated with a gold–palladium target for 45 s in argon medium using a current of 18 mA. The coating thickness for fibers and yarn samples should be 160–190 Å, as a thin layer would not reduce charging enough, and the thick layer would obscure surface details. SEM photomicrographs were taken with cold field-emission scanning electron microscope HITACHI S-4300 to determine the eventual fibers surface and cross section morphology.

Thermal shrinkage

The thermal-shrinkage test was carried out using the Testrite Thermal shrinkage Oven, MK IV Thermal shrinkage-Force Tester from Testrite, UK. The instrument comprises of the heating chamber zone (250 × 110 × 80 mm), temperature controller, computer microprocessor, L.E.D readouts for results, and the sliding carriage, which afford the means of mounting the test sample and presenting it to the heated zone, plus a load cell, and free thermal shrinkage attachment. The loaded threads carrier consisted of a jaw/clamp on one end and the free thermal shrinkage drum with low-torque potentiometer fitted to give the results on the other end. Using a load cell of 10 g and thermal-shrinkage pot, the computer microprocessor determines the results shown on the front display panel, and the movement expressed as

TABLE II
L32 Experimental Design Array for the Spinning Experiment

Trial number	T	MPS	QA	SF	WS
1	145	12	50	0.5	50
2	130	6	50	0.5	50
3	145	12	50	0.5	100
4	145	12	50	0.35	100
5	130	6	50	0.35	100
6	130	12	35	0.5	50
7	145	6	35	0.5	50
8	145	6	50	0.5	50
9	130	6	35	0.5	100
10	130	6	50	0.35	50
11	130	6	35	0.35	100
12	145	12	50	0.35	50
13	145	12	35	0.5	100
14	145	12	35	0.35	50
15	130	12	50	0.35	100
16	130	12	50	0.5	50
17	130	6	50	0.5	100
18	130	12	50	0.35	50
19	145	6	50	0.35	100
20	130	6	35	0.5	50
21	145	6	50	0.35	50
22	145	6	50	0.5	100
23	130	12	50	0.5	100
24	130	12	35	0.35	100
25	130	6	35	0.35	50
26	145	12	35	0.35	100
27	145	12	35	0.5	50
28	145	6	35	0.35	100
29	130	12	35	0.35	50
30	145	6	35	0.5	100
31	130	12	35	0.5	100
32	145	6	35	0.35	50

a % of the sample length is related to thermal shrinkage/extension under a constant tension during heating. Samples were heated for 2 min at 60°C. The thermal shrinkage is calculated as $100 \times (L_0 - L_1)/L_0$, where L_0 is original sample length and L_1 is thermal shrinkage/extension sample length under a constant tension. The factors affecting the results are sample weighting, operating temperature, duration of test, and count of samples.

RESULTS AND DISCUSSION

In one block, a fraction factorial experimental design (L32) with random order was used for the 32 screening trials involving five control parameters T, MPS, QA, SF, and WS with two levels for each parameter as shown in Table II. The standard order of the trial's number of the matrix design should be randomly assigned by used software. The detailed experimental arrangement of the trials and the calculated results of diameter, tenacity, elongation at break, modulus, and thermal shrinkage are shown in Table III. The cross section shape of the produced fibers depends on the shape of spinneret nozzles and the spinning method. That shape will affect on the luster, bulk, body texture, and hand of end use fibers. In terms of influence of the process parameters on the filament the surface microstructure and cross section, Figure 2 shows an SEM photomicrograph of fibers' surface and cross section. Fibers have a circular cross section with uniform surface, which agreed with previous results.

The relationship between several numeric variables was analyzed by performing various statistical and graphical analyses to obtain the multiple-variable analysis, which gives interesting views into the data. Multiple-variable analysis allows calculating specific summary statistics taking into account many factors, such as standard deviations and average, confidence intervals, correlations, and covariance. Figure 3 shows multiple-variable analysis among studied parameters; diameter, tenacity, elongation at break, modulus, and thermal shrinkage of AAC as-spun fibers.

Statistical analysis of the effects of the factors and their interactions on the responses

As a two-level experiment, a factor effect and interaction effect could be determined as the difference between the average responses at the low and the high level of the studied factors (Table I). A Pareto chart shows the significant arrangement of factors and their interactions in decreasing order (y-axis) depending on the significant effect (x-axis). The Pareto chart is a means of effect estimate plotting similar to a horizontal diagram, and factors can have a positive (+) or negative (−) effect. The order of the significance of the factors is presented for each response, and more interesting details will be described in the following statistical analysis to show the importance and the direction of the effect and the way that the factors interact with each other. Pareto charts (Fig. 4) for diameter (a), tenacity (b), elongation at break (c), modulus (d), and thermal shrinkage (e) show the significant arrangement of factors and their interactions in decreasing order. The Pareto chart for diameter [Fig. 4(a)] clearly shows that winding speed, metering speed, their interaction, and extrusion temperature are the most important factors affecting the diameter. The Pareto chart for tenacity [Fig. 4(b)] clearly shows that extrusion temperature, metering pump speed, winding speed, and the interaction between them are the most important factors affecting the tenacity followed by other factors and interactions. The Pareto chart for elongation at break [Fig. 4(c)] clearly shows that winding speed, metering pump speed, extrusion speed, quench air speed, and the interactions (T and SF, MPS and WSB, and MPS and SF) are the most important factors affecting the elongation at break

TABLE III
Responses Data of Diameter, Tenacity, Elongation, Modulus, and Thermal Shrinkage for the Experiment of Spinning of AAC

Trial number	Count den	Tenacity (g/den)	Elongation (%)	Modulus (g/den)	Diameter (μm)	Thermal shrinkage (%)
1	3079.5	0.351	910	0.181	109.2	−0.50
2	1878.6	0.285	600	0.163	85.3	−0.25
3	1445.7	0.422	605	0.194	74.8	−1.00
4	1569.3	0.405	640	0.192	77.9	−1.20
5	963.9	0.358	420	0.273	61.1	−0.83
6	3133.5	0.32	900	0.196	110.1	+0.17
7	1630.8	0.38	766	0.182	79.4	−1.00
8	1738.8	0.42	700	0.189	82.0	−0.75
9	915.9	0.338	390	0.227	59.5	−0.58
10	1900.8	0.284	572	0.176	85.8	+0.00
11	904.2	0.327	380	0.237	59.1	+0.33
12	2928.9	0.369	876	0.178	106.5	+0.00
13	1493.4	0.415	728	0.210	76.0	−1.25
14	3030.3	0.371	976	0.181	108.3	−0.15
15	1691.4	0.34	570	0.197	80.9	+0.00
16	3219	0.318	860	0.163	111.6	−0.25
17	923.7	0.347	386	0.301	59.8	−0.25
18	3198.6	0.331	924	0.176	111.2	+0.57
19	909.6	0.649	390	0.244	59.3	−1.58
20	1819.2	0.29	594	0.236	83.9	+0.00
21	1813.5	0.391	668	0.158	83.8	−1.00
22	845.1	0.651	460	0.277	57.2	−2.17
23	1753.2	0.308	556	0.223	82.4	+0.00
24	1597.2	0.334	662	0.224	78.6	−0.17
25	1842.3	0.301	638	0.221	84.4	0.00
26	1581.6	0.392	706	0.179	78.2	−0.83
27	2872.8	0.369	970	0.176	105.4	−0.17
28	834.9	0.623	412	0.231	56.8	−2.17
29	3204	0.321	964	0.163	111.3	+1.00
30	926.1	0.486	673	0.228	59.9	−2.17
31	1683.3	0.33	630	0.221	80.7	+0.00
32	1596	0.397	670	0.182	78.6	−1.42

followed by the interactions (T and MPS and T and QA) and other factors and interactions. The Pareto chart for modulus in Figure 4(d) shows that winding speed, metering pump speed, extrusion temperature, spin finish application, and the interactions (QA and WS, MPS and WS, T and QA, MPS and QA, and T

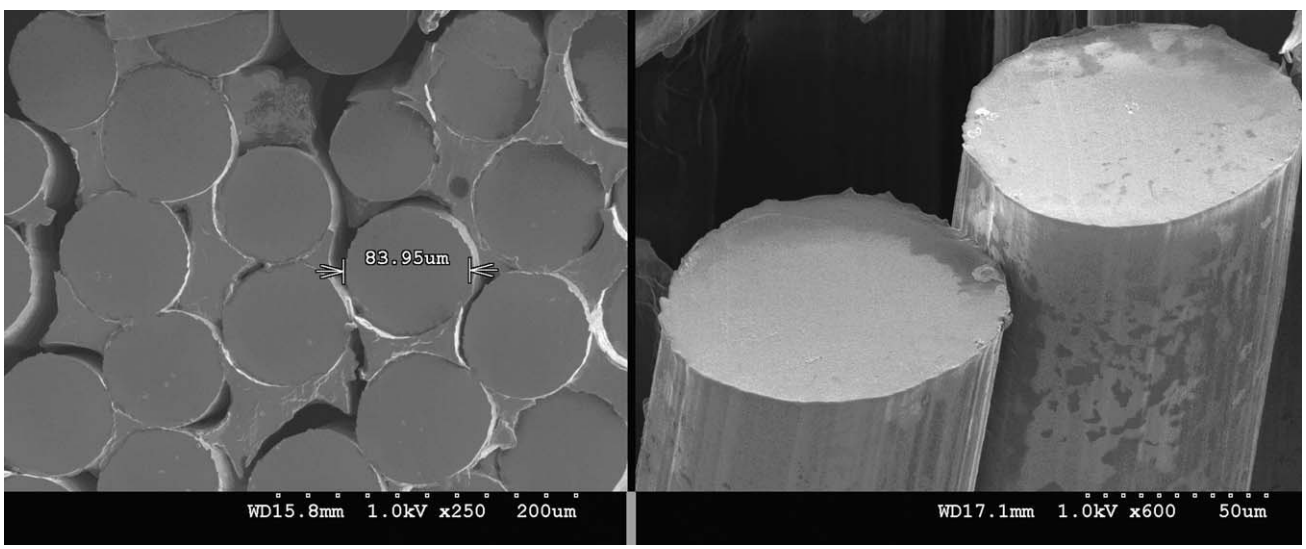

Figure 2 SEM photo of AAC fibers' surface and cross section.

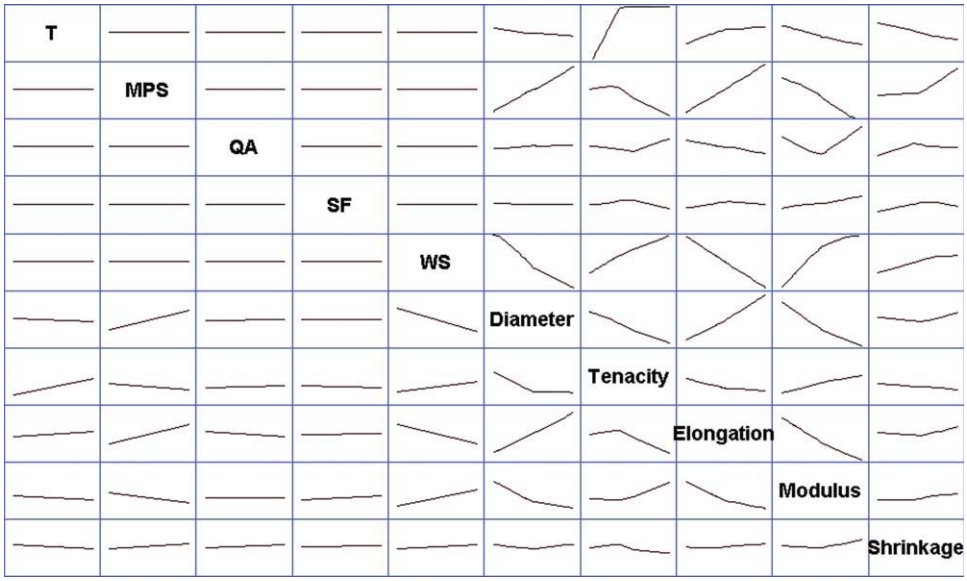

Figure 3 Multiple-variable analysis between the studied parameters, diameter, tenacity, elongation at break, modulus, and thermal shrinkage of AAC spun fibers. [Color figure can be viewed in the online issue, which is available at wileyonlinelibrary.com.]

and WS) are the most important factors affecting the modulus followed by the interactions (T and MPS and SF and WS) and other factors and interactions. The Pareto chart for thermal shrinkage [Fig. 4(e)] clearly shows that extrusion temperature, winding speed, metering pump speed, spin finish application, and the interactions (T and WS, T and MPS, and T and QA) are the most important factors affecting the thermal shrinkage followed other factors and interactions.

Plots in Figure 5(a–j) show the main effects and the interaction plots caused by the main factors and their interactions on the diameter, tenacity, elongation at break, modulus, and thermal shrinkage of as-spun fibers.

In main effects plots, for example, Figure 5(b), the factor effect between the average responses of the low and high level of the factors is presented, and the capital letters along the horizontal axis represent the main factors and their interactions. The effect line determines the effect of the factors from the slope of the line between the two levels. The steeper the slop, the more significant is the factor effect. The direction of the effect is determined by the slope of the line, and a positive effect is obtained when the line increases from the left to the right and vice versa.

The interaction plot, for example, Figure 5(b), is a useful practice used to determine the interaction between each two factors. The first interaction factor is presented on the *x*-axis with low and high levels. The second interaction factor is presented as two different lines for low and high levels; the *Y*-axis shows the averages of the measured responses. If the angle between the interaction lines is very small or the interaction lines are parallel, the interaction is not significant.

Statistical analysis of the effects caused by the main factors effect, and their interactions on diameter [Fig. 5(a,b)] show that the effects from the temperature WS, MPS, T, and the interaction between winding speed and metering pump speed are significant. The interaction between winding speed and metering pump speed is related to the relationship between the output of the machine and the collection at different speeds, which affect the throughput flow rate and the spin draw ratio of the filaments to reduce the filament diameter. The main factors effect for tenacity [Fig. 5(c–d)] is strongly affected by extrusion temperature, winding speed, and metering pump speed. The interactions T and MPS, T and WS, and WS and MPS are significant. The interactions QA and WS and SF and WS need to be further investigated. No significant effect has been reported for other factors and interactions. Elongation at break [Fig. 5(e–f)] was affected by winding speed, metering pump speed, quench air speed, and extrusion temperature. The interactions T and SF, MPS and SF, MPS and WS, and T and MPS need to be further investigated, and there is no significant effect that has been reported for other factors and interactions.

Modulus [Fig. 5(g,h)] was affected by main factors metering pump speed and winding speed and extrusion temperature. Interactions MPS and WS and QA and WS affect the modulus, and T and QA are on the borderline of significance and need to be investigated. Thermal shrinkage [Fig. 5(i,j)] is strongly

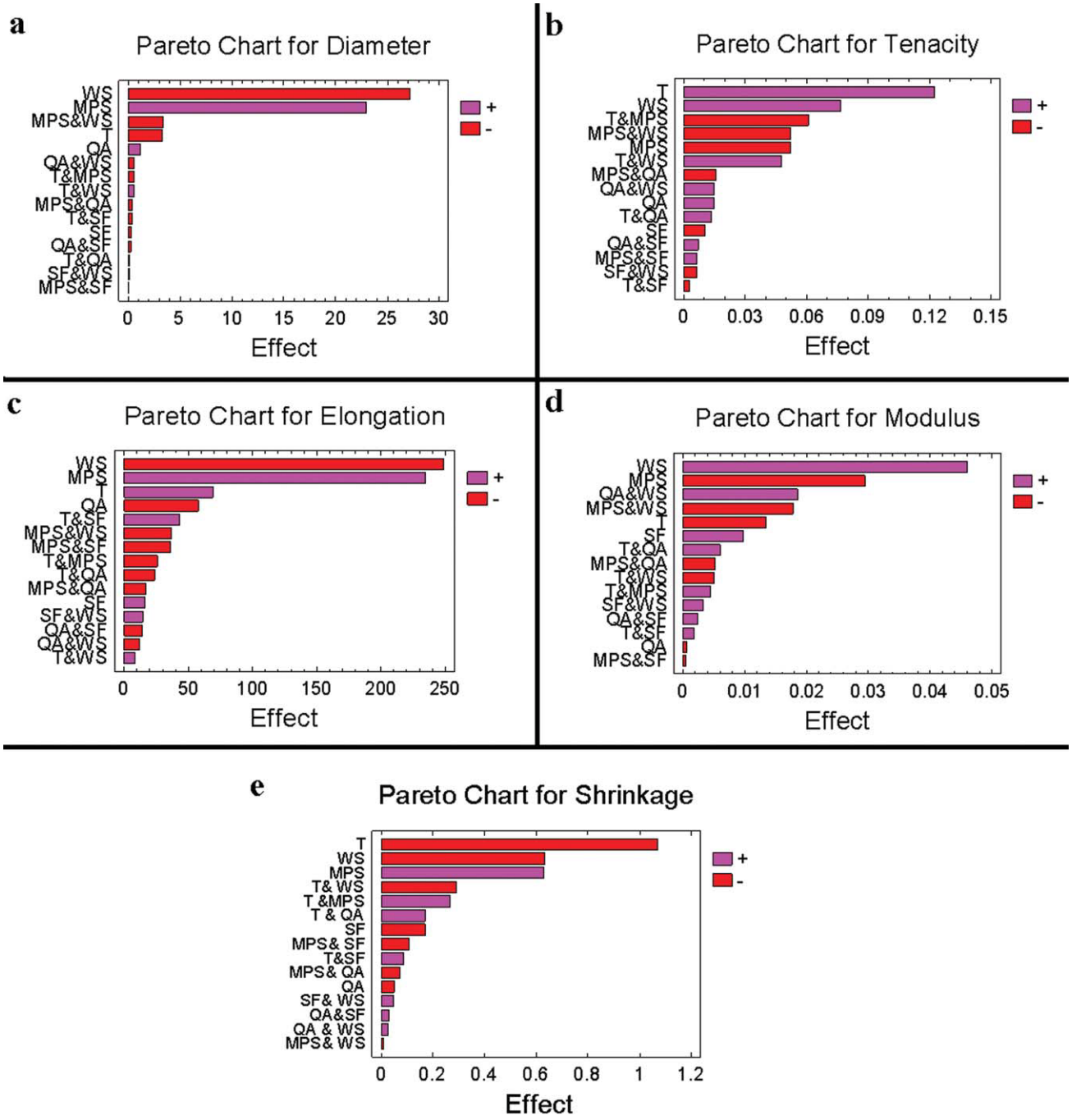

Figure 4 A ranked list of significant arrangement effects and interactions for diameter, tenacity, elongation at break, modulus, and thermal shrinkage (Pareto chart). [Color figure can be viewed in the online issue, which is available at wileyonlinelibrary.com.]

affected by extrusion temperature, winding speed, and metering pump speed. The interactions T and MPS and T and WS strongly affect the thermal shrinkage and need to be further investigated. All previous factors and interactions, which are on the borderline of significance, can be adjusted later using ANOVA.

As an alternative to an effect plot, a normal probability plot or a Daniel's plot shows the percentage and standardized effects and can be used to assess the significance of the factors' effects.[24] The straight line represents the empirical principle in the middle of the range; the significant effect for both positive and negative effects could be reflected in deviation of the data points from the straight line. The further the deviation, the greater the statistical significance. Figure 6 displays the normal probability plots for on the diameter, tenacity, elongation at break, modulus,

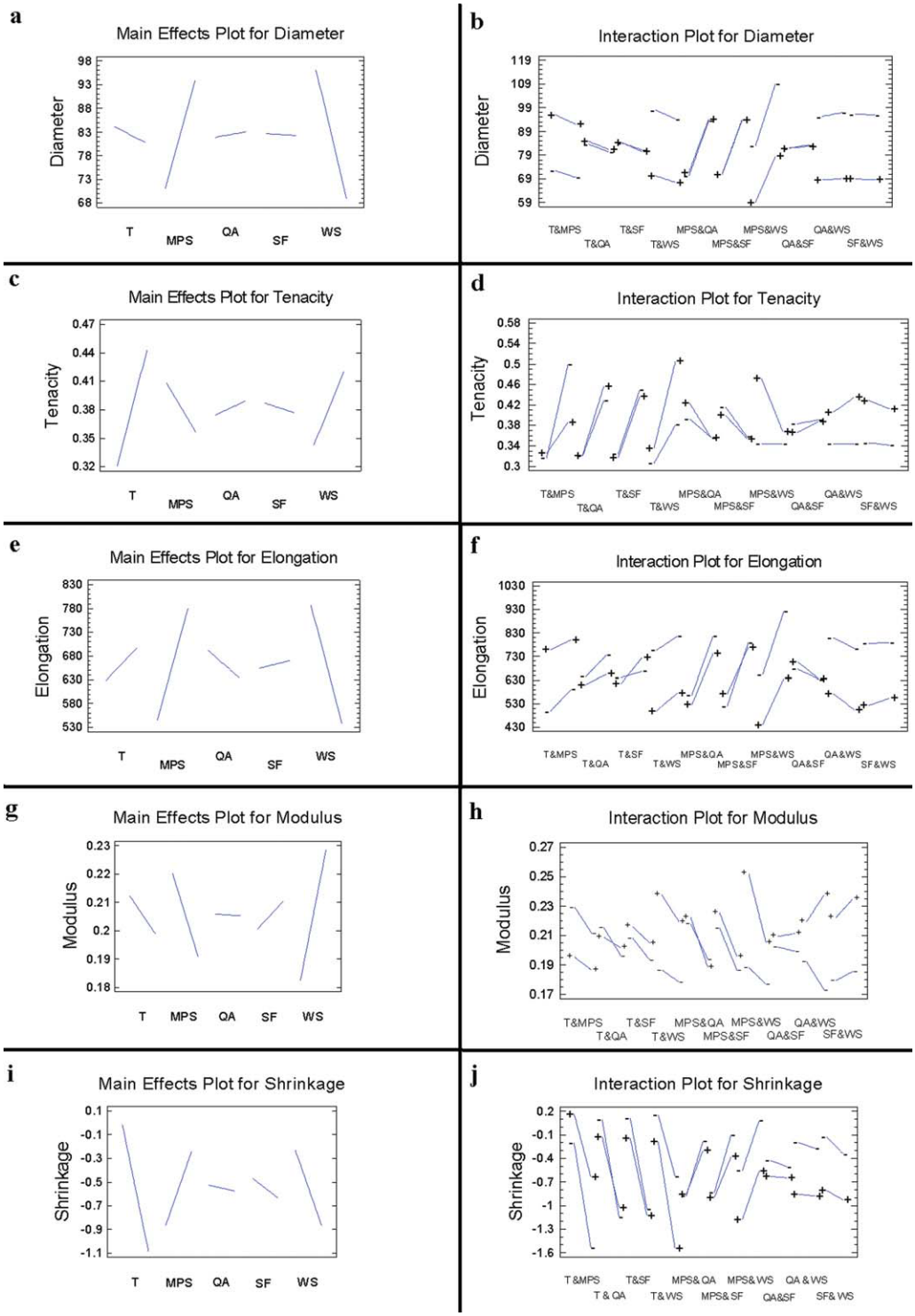

Figure 5 The main affect and interaction plots for diameter, tenacity, elongation at break, modulus, and thermal shrinkage. [Color figure can be viewed in the online issue, which is available at wileyonlinelibrary.com.]

and thermal shrinkage of as-spun fibers obtained using the design matrix and shows the percentage and standardized effects. The diameter plot [Fig. 6(a)] shows the clear effect of metering pump speed, winding speed, and their interaction on the diameter. Other effects appear from extrusion temperature and quench air speed, which could be related to the effect of these factors on the down draw ratio as has been noted in previous work.[44] Tenacity [Fig. 6(b)] is affected by extrusion temperature, winding speed, metering pump speed, and their interactions T and MPS, T and WS, and WS and MPS. Together with the main effects of extrusion temperature, winding speed, and metering pump speed, the interactions (T

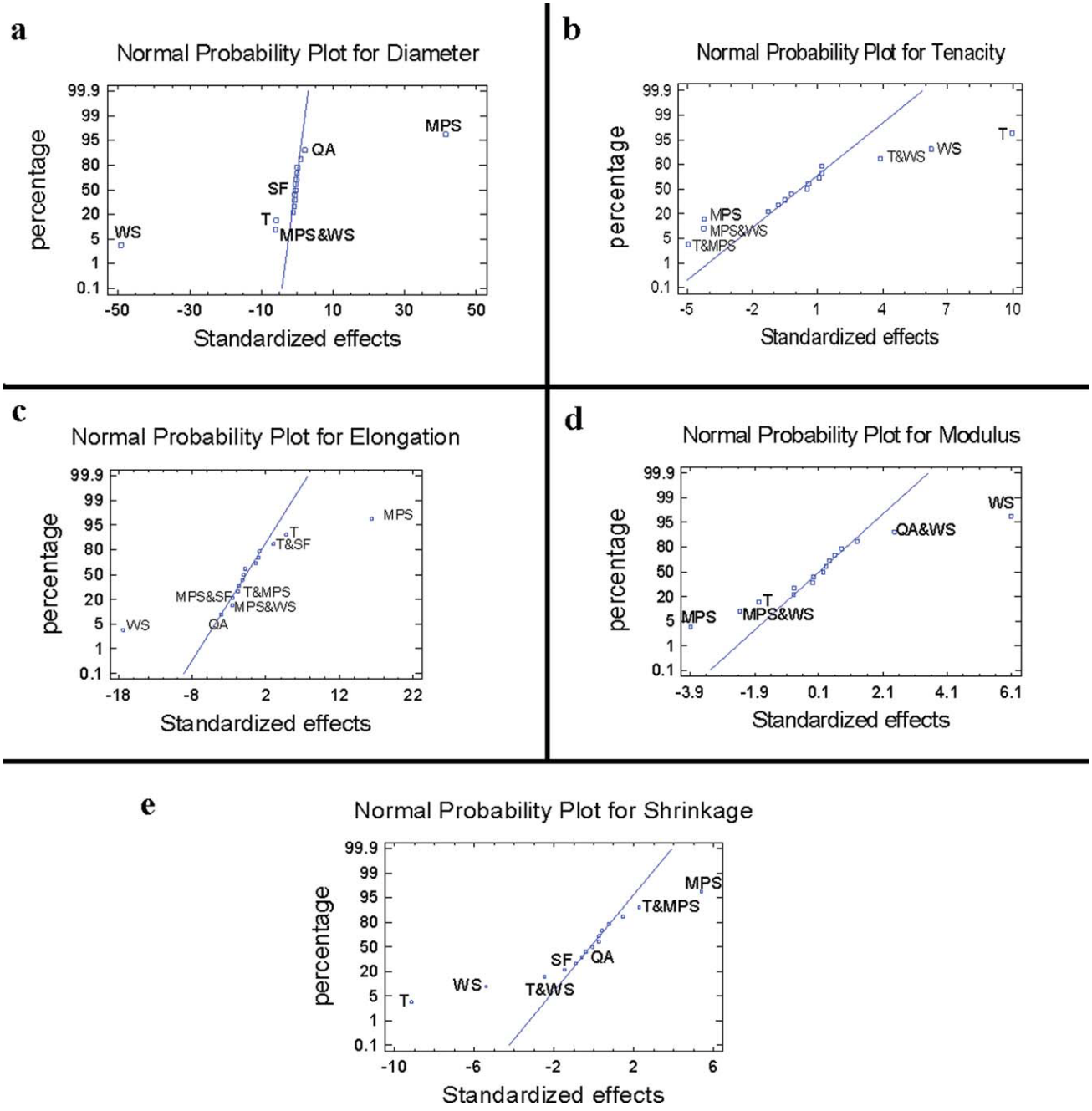

Figure 6 Statistical standardized and percentage order values of factors and their interactions for the diameter, tenacity, elongation at break, modulus, and thermal shrinkage (the normal probability plot). [Color figure can be viewed in the online issue, which is available at wileyonlinelibrary.com.]

and SF and MPS and WS) affect the elongation at break [Fig. 6(c)], which can be related to the friction effect on the spin draw ratio, which decreases the elongation at break ratio. In the modulus analysis [Fig. 6(d)], winding speed, metering pump speed, extrusion temperature, and the interactions (MPS and WS and QA and WS) have the significant effects on the modulus. The thermal shrinkage is affected by extrusion temperature, winding speed, metering pump speed, and the interactions (T and WS and T and MPS), respectively, as was been shown in Figure 6(e).

Analysis of variance

To determine the factor effects in terms of statistical significance, analysis of variance (ANOVA) of the data was conducted. The ANOVA method, designed by Sir R. A. Fisher,[48] is a mathematical method comparing the response data to the error data and then

TABLE IV
ANOVA Results Identifying the Statistical Significance of Factors Effects on the Diameter, Tenacity, Elongation, Modulus, and Shrinkage

	Diameter		Tenacity		Elongation		Modulus		Shrinkage	
Source	F	P	F	P	F	P	F	P	F	P
T	35.3	0.000	99.3	0.000	23.3	0.000	3.2	0.095	83.7	0.000
MPS	1727.0	0.000	17.9	0.001	269.9	0.000	15.1	0.001	29.0	0.000
QA	4.2	0.056	1.4	0.249	16.3	0.001	0.0	0.942	0.2	0.674
SF	0.3	0.596	0.7	0.419	1.3	0.269	1.6	0.219	2.1	0.165
WS	2417.5	0.000	39.0	0.000	303.0	0.000	37.1	0.000	29.3	0.000
T and MPS	1.0	0.338	24.6	0.000	3.3	0.089	0.3	0.566	5.2	0.037
T and QA	0.1	0.801	1.2	0.290	2.8	0.114	0.6	0.435	2.1	0.165
T and SF	0.5	0.490	0.1	0.830	9.1	0.008	0.1	0.814	0.6	0.465
T and WS	0.9	0.346	15.1	0.001	0.4	0.559	0.5	0.513	6.2	0.025
MPS and QA	0.6	0.458	1.6	0.220	1. 35	0.262	0.5	0.503	0.4	0.544
MPS and SF	0.0	0.924	0.3	0.607	6.4	0.022	0.0	0.955	0.9	0.371
MPS and WS	36.9	0.000	18.1	0.001	6.5	0.021	5.5	0.032	0.0	0.950
QA and SF	0.2	0.673	0.3	0.573	1.0	0.335	0.1	0.752	0.1	0.809
QA and WS	1.1	0.304	1.4	0.249	0.7	0.431	6.0	0.026	0.1	0.825
SF and WS	0.0	0.901	0.3	0.621	1.1	0.319	0.2	0.667	0.2	0.682

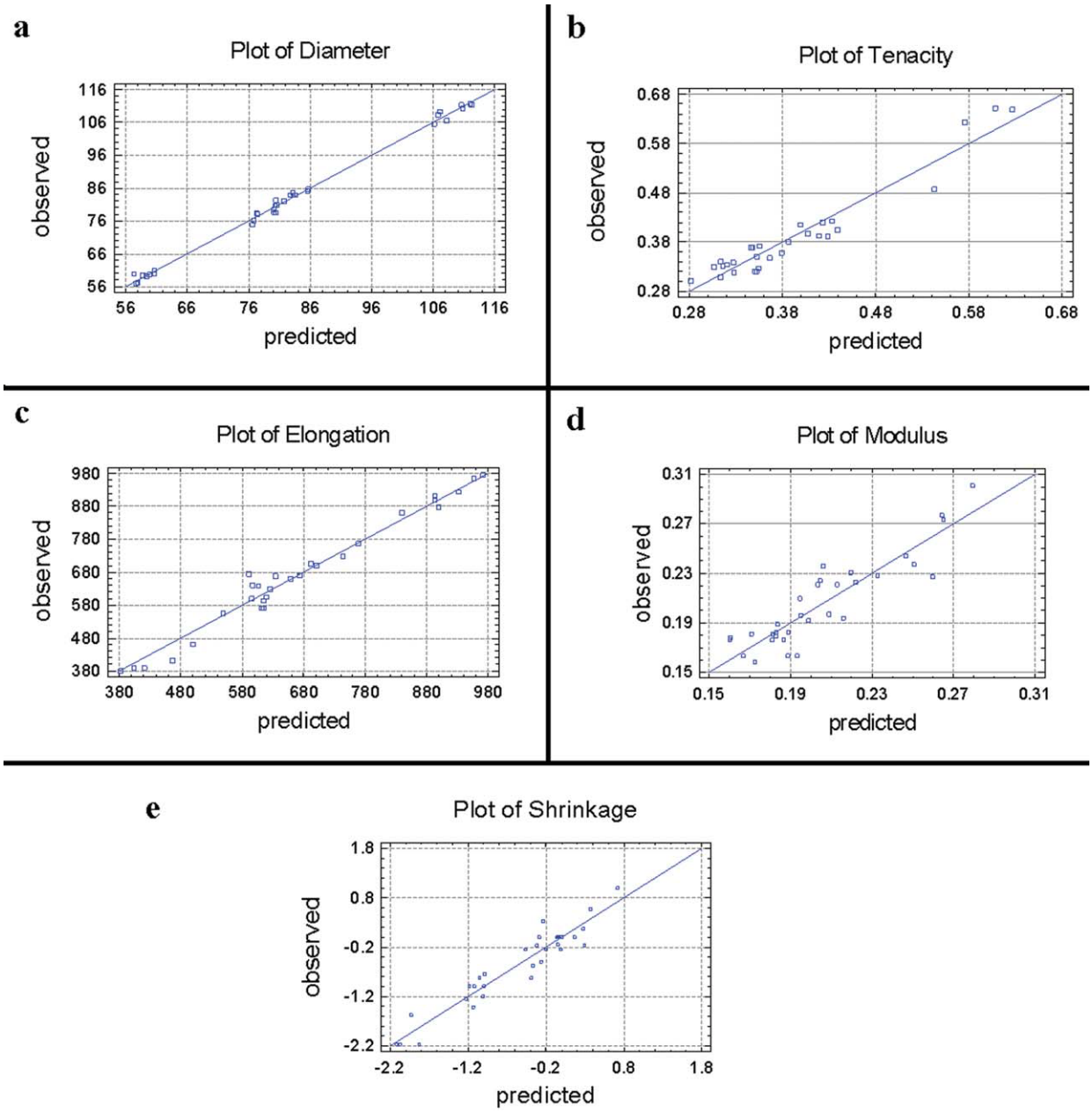

Figure 7 Experimental observed results and theoretical fitted results plots for diameter, tenacity, elongation at break, modulus, and thermal shrinkage. [Color figure can be viewed in the online issue, which is available at wileyonlinelibrary.com.]

determines the significant effect of the independent factors or their interaction. ANOVA partitions the variability in response into separate parts for each effect and tests the statistical significance of each effect by comparing the mean square against the experimental error. A probability or *P*-value ($P \equiv \alpha$-significance level) used in ANOVA provides quantitative and objective criteria for judging the statistical significance of the effects. In case the *P*-values less than 0.05, factor effects are significantly different from zero at the 95.0% confidence level. If the *F*-ratio, a new statistic in ANOVA is greater than the circuital value, the factor has significant effect. $F = 4.49$ is obtained from *F* tables at the appropriate level $\alpha = 0.05$.[48,49] An error could come from either assignable causes that is variation due to changes in the independent factors or random causes, that is, uncontrolled variation. ANOVA results for diameter, tenacity, elongation at break, modulus, and thermal shrinkage of as-spun fibers are listed in Table IV. The significance of factors on the diameter is winding speed ($P_{WS} = 0.000$) > metering pump speed ($P_{MPS} = 0.000$) > extrusion temperature ($P_T = 0.000$). No significant effect of spin finish application and quench air was found. The interaction between metering pump speed and winding speed has a significant effect ($P_{MPS\ and\ WS} = 0.000$). There are no significant effects of the other interactions on diameter.

Of the mechanical properties, tenacity is significantly affected by extrusion temperature ($P_T = 0.000$) > winding speed ($P_{WS} = 0.000$) > metering pump speed ($P_{MPS} = 0.001$) and the interaction between extrusion temperature and metering pump speed ($P_{T\ and\ MPS} = 0.000$) > the interaction between metering pump speed and winding speed ($P_{MPS\ and\ WS}$ 0.001) > the interaction between extrusion temperature and winding speed ($P_{T\ and\ WS} = 0.001$). There are no significant effects of the other factors and interactions. Elongation at break is significantly affected by winding speed (P_{WS} 0.000) > metering pump speed ($P_{MPS} = 0.000$) > extrusion temperature ($P_T = 0.000$) > quench air speed ($P_{QA} = 0.001$) and the interaction between extrusion temperature and spin finish application ($P_{T\ and\ SF} = 0.008$) > the interaction between metering pump speed and winding speed ($P_{MPS\ and\ WS} = 0.021$) > the interaction between metering pump speed and spinning finish application ($P_{MPS\ and\ SF} = 0.022$). There are no significant effects of the other factors and interactions. Modulus is significantly affected by winding speed (P_{WS} 0.000) > metering speed ($P_{MPS} = 0.001$) the interaction between quench air speed and winding speed ($P_{QA\ and\ WS} = 0.026$) > the interaction between metering pump speed and winding speed ($P_{MPS\ and\ WS} = 0.032$). There are no significant effects of the other factors and interactions. Thermal shrinkage is significantly affected by extrusion temperature ($P_T = 0.000$) > winding speed (P_{WS} 0.000) > metering pump speed ($P_{MPS} = 0.000$), the interaction extrusion temperature and winding speed ($P_{T\ and\ WS} = 0.025$) > the interaction extrusion temperature and metering pump speed ($P_{T\ and\ MPS} = 0.037$). There are no significant effects of the other factors and interactions.

The regression equation and estimation results

Based on the analysis, a simplified model was fitted by the regression equation, which has been fitted to the experimental data. The regression equations enhanced form the main source code in the enhanced forecasting program presenting the melt-spinning process of aromatic–aliphatic copolyester fibers. In terms of the coded values (Table I), the regression eqs. (1–5) for diameter, tenacity, elongation at break, modulus, and thermal shrinkage are given as follows:

$$\begin{aligned}\text{Diameter} &= 61.3105 - 0.0162222^{*}\text{T} + 7.61583^{*}\text{MPS} \\ &+ 0.539278^{*}\text{QA} + 54.3222^{*}\text{SF} - 0.479967^{*}\text{WS} \\ &- 0.0121111^{*}\text{T}^{*}\text{MPS} - 0.00125556^{*}\text{T}^{*}\text{QA} \\ &- 0.346667^{*}\text{T}^{*}\text{SF} + 0.00143^{*}\text{T}^{*}\text{WS} - \\ &0.00933333^{*}\text{MPS}^{*}\text{QA} - 0.119444^{*}\text{MPS}^{*}\text{SF} \\ &- 0.0223667^{*}\text{MPS}^{*}\text{WS} - 0.211111^{*}\text{QA}^{*}\text{SF} \\ &- 0.00156333^{*}\text{QA}^{*}\text{WS} + 0.0186667^{*}\text{SF}^{*}\text{WS} \quad (1)\end{aligned}$$

$$\begin{aligned}\text{Tenacity} &= -0.724049 + 0.00675139^{*}\text{T} + 0.212372^{*}\text{MPS} \\ &- 0.0179125^{*}\text{QA} - 0.01125^{*}\text{SF} - 0.0137837^{*}\text{WS} \\ &- 0.00135417^{*}\text{T}^{*}\text{MPS} + 0.000119444^{*}\text{T}^{*}\text{QA} \\ &- 0.00238889^{*}\text{T}^{*}\text{SF} + 0.000127167^{*}\text{T}^{*}\text{WS} \\ &- 0.000348611^{*}\text{MPS}^{*}\text{QA} + 0.0143056^{*}\text{MPS}^{*}\text{SF} \\ &- 0.000347917^{*}\text{MPS}^{*}\text{WS} + 0.00627778^{*}\text{QA}^{*}\text{SF} \\ &+ 0.0000391667^{*}\text{QA}^{*}\text{WS} - 0.00165^{*}\text{SF}^{*}\text{WS} \quad (2)\end{aligned}$$

$$\begin{aligned}\text{Elongation at break} &= -128.163 + 0.828917^{*}\text{T} \\ &+ 186.364^{*}\text{MPS} + 36.3343^{*}\text{QA} - 4184.63^{*}\text{SF} \\ &- 6.27401^{*}\text{WS} - 0.575^{*}\text{T}^{*}\text{MPS} - 0.212222^{*}\text{T}^{*}\text{QA} \\ &+ 38.2589^{*}\text{T}^{*}\text{SF} + 0.0227767^{*}\text{T}^{*}\text{WS} - 0.369444^{*}\text{MPS}^{*}\text{QA} \\ &- 80.4639^{*}\text{MPS}^{*}\text{SF} - 0.243608^{*}\text{MPS}^{*}\text{WS} \\ &- 12.63^{*}\text{QA}^{*}\text{SF} - 0.0307767^{*}\text{QA}^{*}\text{WS} + 3.922^{*}\text{SF}^{*}\text{WS} \quad (3)\end{aligned}$$

$$\begin{aligned}\text{Modulus} &= 0.766958 - 0.00374583^{*}\text{T} - 0.00424653^{*}\text{MPS} \\ &- 0.0110431^{*}\text{QA} - 0.306528^{*}\text{SF} + 0.00136708^{*}\text{WS} \\ &+ 0.0000986111^{*}\text{T}^{*}\text{MPS} + 0.0000538889^{*}\text{T}^{*}\text{QA} + \\ &0.00161111^{*}\text{T}^{*}\text{SF} - 0.0000135^{*}\text{T}^{*}\text{WS} \\ &- 0.000115278^{*}\text{MPS}^{*}\text{QA} - 0.000972222^{*}\text{MPS}^{*}\text{SF} - \\ &0.00011875^{*}\text{MPS}^{*}\text{WS} + 0.00216667^{*}\text{QA}^{*}\text{SF} \\ &+ 0.0000495^{*}\text{QA}^{*}\text{WS} + 0.000883333^{*}\text{SF}^{*}\text{WS} \quad (4)\end{aligned}$$

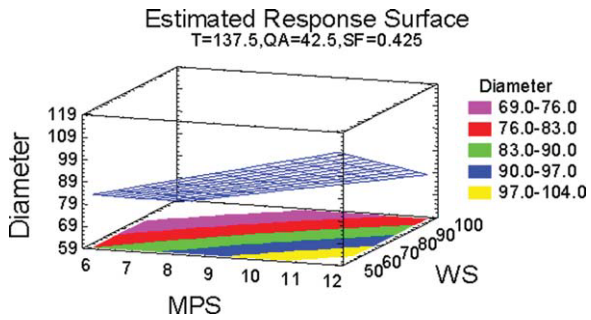

Figure 8 Estimated response surface between MPS and WS for diameter. [Color figure can be viewed in the online issue, which is available at wileyonlinelibrary.com.]

$$\begin{aligned}\text{Thermal shrinkage} &= 22.1331 - 0.163778^{*}\text{T} \\ &- 0.535^{*}\text{MPS} - 0.212722^{*}\text{QA} - 11.7389^{*}\text{SF} \\ &+ 0.0856333^{*}\text{WS} + 0.00591667^{*}\text{T}^{*}\text{MPS} \\ &+ 0.00151111^{*}\text{T}^{*}\text{QA} + 0.0777778^{*}\text{T}^{*}\text{SF} - \\ &0.000773333^{*}\text{T}^{*}\text{WS} - 0.00161111^{*}\text{MPS}^{*}\text{QA} \\ &- 0.238889^{*}\text{MPS}^{*}\text{SF} - 0.00005^{*}\text{MPS}^{*}\text{WS} + \\ &0.0255556^{*}\text{QA}^{*}\text{SF} + 0.00007^{*}\text{QA}^{*}\text{WS} + 0.013^{*}\text{SF}^{*}\text{WS}\end{aligned} \quad (5)$$

For the observed results and fitted results generated for each trial, the models gave acceptable results for the diameter [Fig. 7(a)], tenacity [Fig. 7(b)] and elongation at break [Fig. 7(c)], modulus (Fig. 7(d)], and thermal shrinkage [Fig. 7(e)].

The model gave acceptable results with small variation for reasons such as blocked nozzles in the spinneret because of the nature of this polymer and the nonuniform flow, the tension variation, some tension during preparing the sample for the test, or the fractional resistance between the fibers that transfers the forces between the fibers and raises the fraction.[35]

Theoretically, the obtained statistical-based models could be tested regarding the reported dynamic modeling of melt-spinning process[34,52] through a set of rate equations. Input and output values should be adjusted as to the material properties and the process conditions. That helps to find the general effect with some numerical differences in regression method's results obtained from such theoretical models.[53]

The pattern of estimated responses is based on the assumed model derived from the experimental observations. The geometric result of plotting a response variable is as a function of two factors, and the interaction appears with the surface twist. The remaining factors are fixed on the middle of their range, for example, $T = 130 + (145–130)/2 = 137.5°C$. If twist is found in the 3D-estimated surface-response diagrams, the detected effect is significant. To determine the direction of the interaction MPS and WS, the estimated response surfaces of

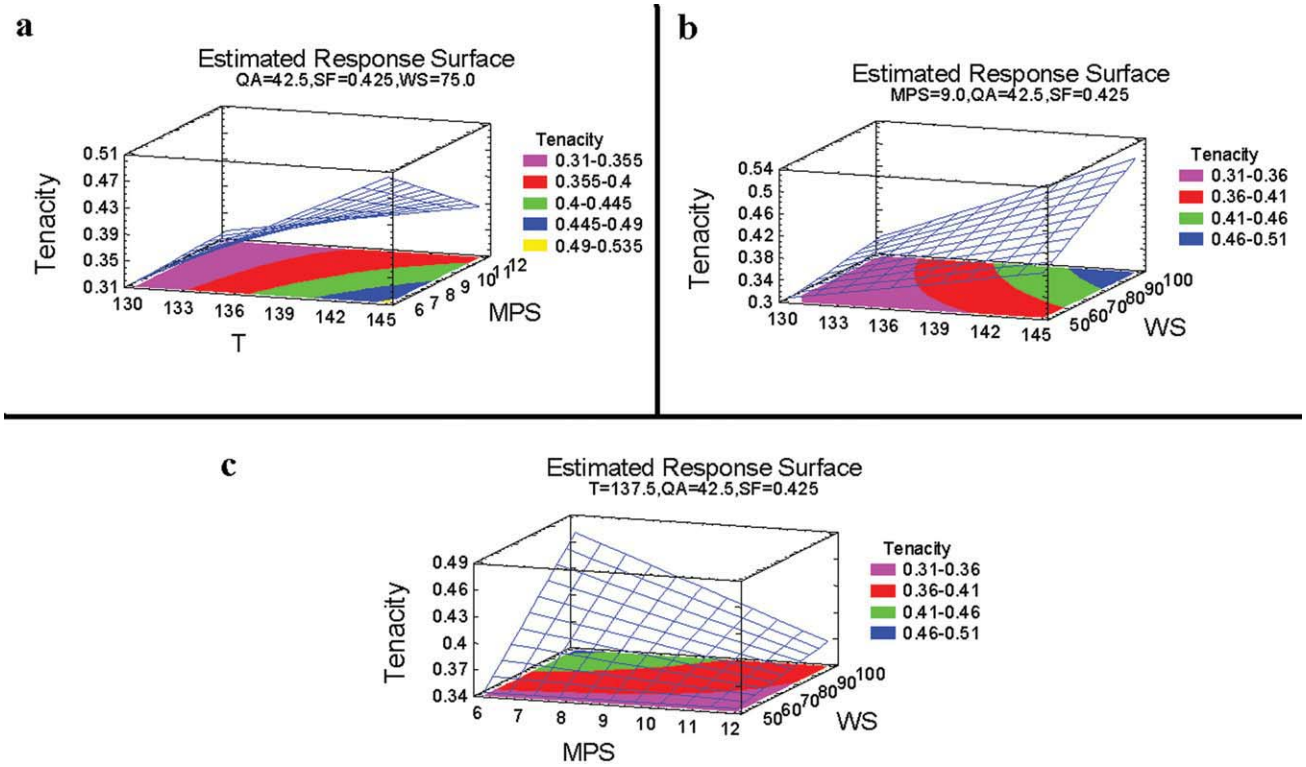

Figure 9 Estimated response surface for tenacity (MPS and T, WS and T, and WS and MPS). [Color figure can be viewed in the online issue, which is available at wileyonlinelibrary.com.]

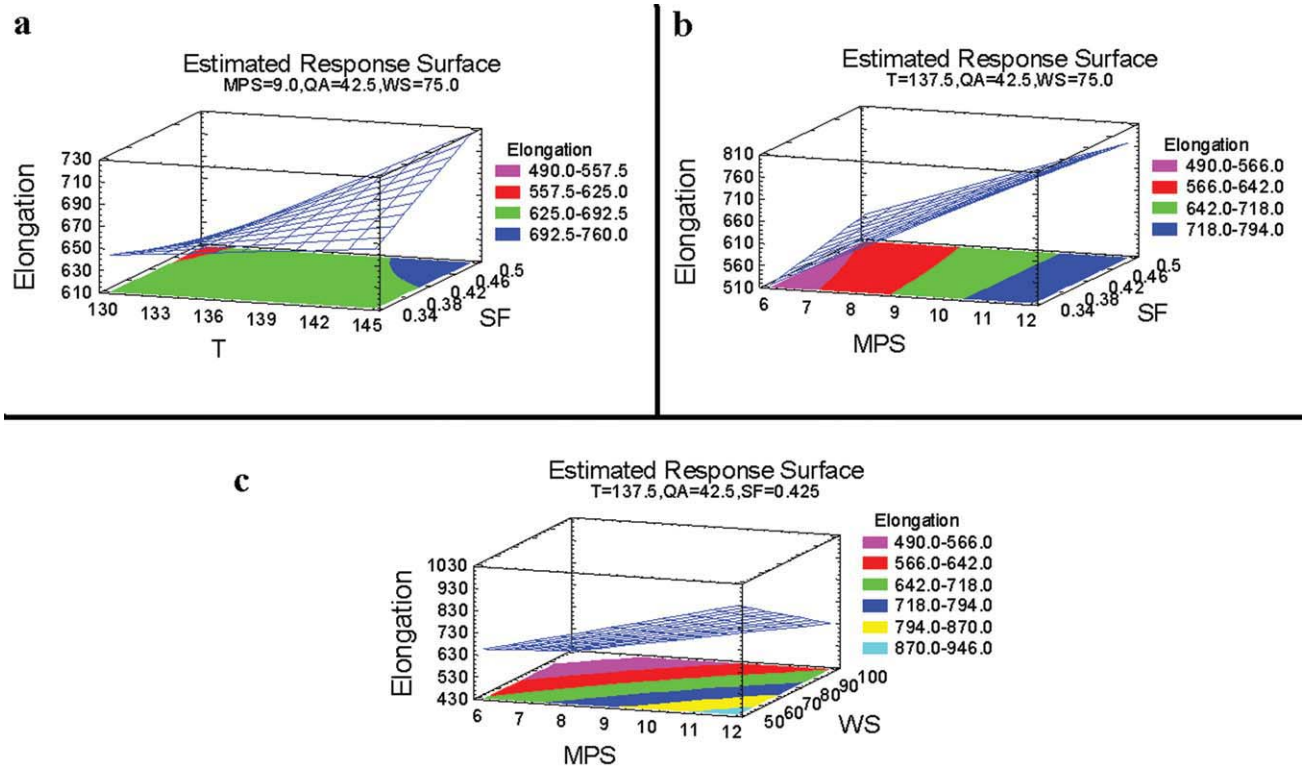

Figure 10 Estimated response surface for elongation at break (SF and T, MPS and SF, and WS and MPS). [Color figure can be viewed in the online issue, which is available at wileyonlinelibrary.com.]

diameter are used as shown in Figure 8. There are three axes, the first interaction factor MPS (metering pump speed) is on the *X*-axis and low and high levels, the second interaction factor WS (winding speed) is on the *Y*-axis with low and high levels, and *Z*-axis shows the averages of the measured diameter. There is small twist found in the surface, and, as a result, a significant effect has been detected between metering pump speed and winding speed, which confirms the previous analysis results. In a similar analysis, the estimated response surfaces for tenacity (Fig. 9), elongation at break (Fig. 10), modulus (Fig. 11), and thermal shrinkage (Fig. 12) show the relationships between them and the previously studied effected interactions. Obtained results agree with the previous analysis conclusions.

Cube plots are used to summarize predicted values for the dependent variable by giving the respective high and low setting of factors. The cube plot shows the predicted values for three factors at a time, and the rest factors are fixed on the middle of their range (the middle level). In the cube plots for the diameter [Fig. 13(a)], tenacity [Fig. 13(b)], elongation at break [Fig. 13(c),] modulus [Fig. 13(d)], and

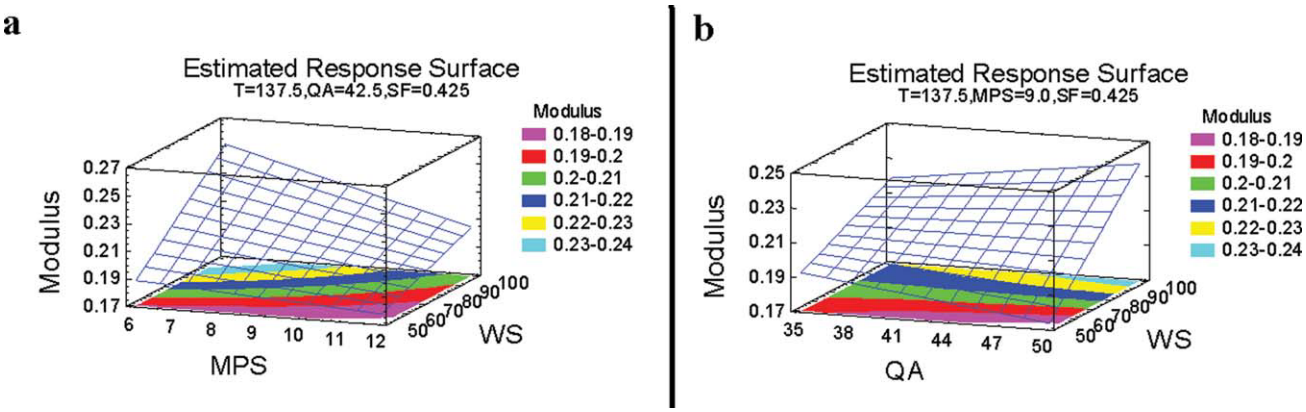

Figure 11 Estimated response surface for modulus (WS and MPS and QA and WS). [Color figure can be viewed in the online issue, which is available at wileyonlinelibrary.com.]

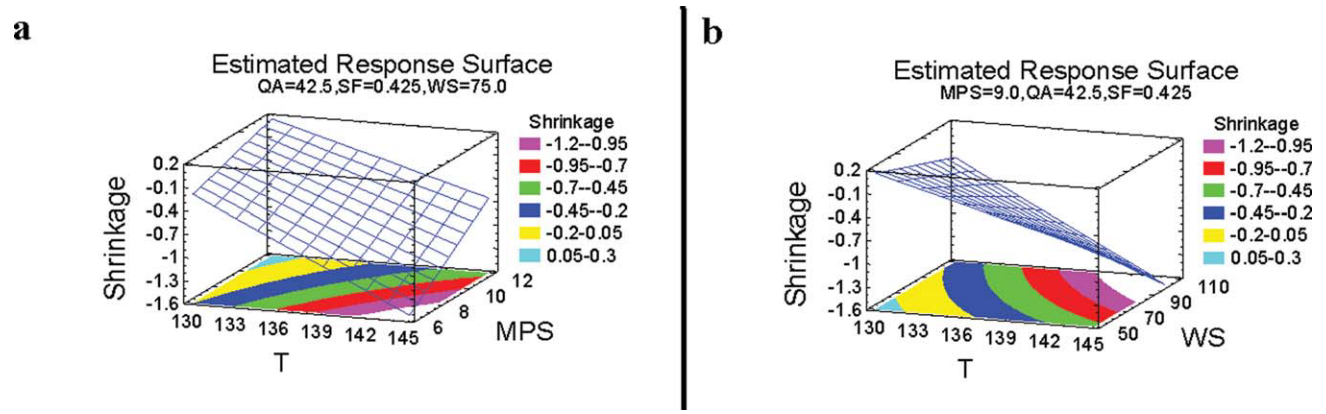

Figure 12 Estimated response surface for thermal shrinkage (MPS and T and WS and T). [Color figure can be viewed in the online issue, which is available at wileyonlinelibrary.com.]

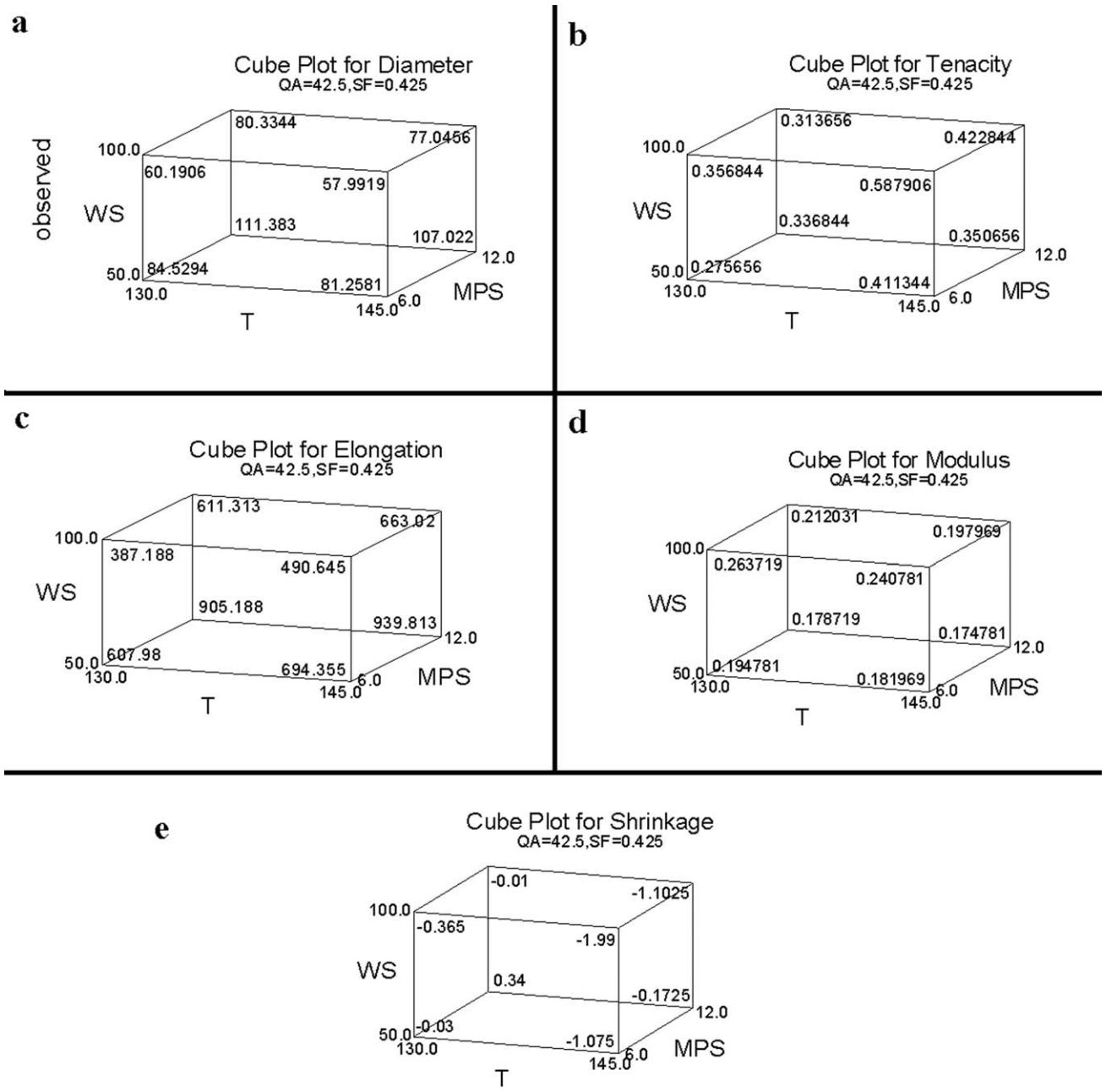

Figure 13 Cube plots of the estimated effects for the high and low settings of MPS, T. and WS for diameter, tenacity, elongation at break, modulus. and thermal shrinkage.

TABLE V
The Combinations of Factor Levels for the Diameter, Tenacity, Elongation, Modulus, and Shrinkage

			The combination of factor levels (↓, low level; ↑, high level)				
Response	Optimum model	Optimum value	T	MPS	QA	SF	WS
Diameter	Maximum	112.239	↓	↑	↑	↓	↓
	Minimum	57.4144	↑	↓	↓	↑	↑
Tenacity	Maximum	0.626375	↑	↓	↑	↓	↑
	Minimum	0.267125	↓	↓	↓	↑	↓
Elongation	Maximum	994.501	↑	↑	↓	↑	↓
	Minimum	367.792	↓	↓	↑	↓	↑
Modulus	Maximum	0.279	↓	↓	↑	↑	↑
	Minimum	0.160	↓	↑	↑	↓	↓
Shrinkage	Maximum	0.720625	↓	↑	↓	↓	↓
	Minimum	−2.12188	↑	↓	↓	↓	↑

thermal shrinkage [Fig. 13(e)] depending on the obtained regression equation, each value corresponds to the values of the experimental factors metering pump speed, extrusion temperature, and winding speed at the middle levels of quench air speed and spin finish application range, which are 42.5 and 0.425, respectively.

CONCLUSIONS

A production process of as-spun biodegradable linear AAC fiber has been optimized. The diameter, tenacity, elongation at break, modulus, and thermal shrinkage of fibers have been characterized and modeled. The models forecast the analyzed responses' values through the optimized window. The high-wind up speed adds tension on filaments from the spinneret through the cooling and solidification stages. Decrease of spinning temperature leads to higher viscosity, higher flow resistance through the spinneret's nozzle, and high-die head pressure. Melt-extrusion temperature, metering pump speed, winding speed, and the interaction between the metering pump and the winding speeds are the most important factors affecting the diameter. Extrusion temperature, winding speed, and metering pump speed are the most important factors affecting the mechanical properties and thermal shrinkage as was been described previously.

Table V summarizes the main conclusion of the results in a concise factorial statistical model. The optimization presents the combination of factor levels that maximize and minimize responses over the indicated region. They cover the identified significant main and interaction factors and specify the combinations of factor levels for enhancing responses of as-spun AAC fibers. The theoretical regression models obtained form the main source code in the enhanced forecasting program, which presents the melt-spinning process of aromatic–aliphatic copolyester fibers. After drawing and preparing, fibers could be used in agricultural, horticultural, and other textile applications as environmentally friendly, economical, energy-saving fibers. Together with previous work,[41,42] current results help to understand the production processing of AAC fibers and provide more technical information for scientists and technologists to use suitable conditions. The achieved models used to calculate various statistics include correlations, covariances, and partial correlations.

The responses of the statistical models derived here can be explained by general extrusion theories and the knowledge of the influence of the involved parameters on the studied responses. The enhanced plot optimizes the process parameters to produce the most satisfactory responses and indicate the factors and responses behavior through the optimization window. The achieved models predict one variable given values of one of more other variables. In addition to creating group trials of data with similar characteristics, developing a predicting method, reducing the number of factors and responses to a small set of meaningful measures, determining which combinations of the factors and responses determine most of the variability in analyzed data, and finding combinations of the factors and responses related to each other.

The authors are indebted to James McVee from School of Textiles and Designs, Heriot-Watt University, Scottish Borders Campus for the appreciated technical support on the SEM and tensile test equipments.

References

1. Li, F.; Xu, X.; Li, Q.; Li, Y.; Zhang, H.; Yu, J.; Cao, A. Polymer Degrad Stab 2006, 91, 1685.
2. Deng, L.-M.; Wang, Y.-Z.; Yang, K.-K.; Wang, X.-L.; Zhou, Q.; Ding, S.-D. Acta Mater 2004, 52, 5871.
3. Park, S. S.; Chae, S. H.; Im, S. S. J Polym Sci Part A: Polym Chem 1998, 36, 147.
4. Kang, H. J.; Park, S. S. J Appl Polym Sci 1999, 72, 593.

5. Park, S. S.; Kang, H. J. Polym J 1999, 31, 238.
6. Kleeberg, I.; Hetz, C.; Kroppenstedt, R. M.; Müller, R.-J.; Deckwer, W.-D. Appl Environ Microbiol 1998, 64, 1731.
7. Kang, H. J.; Park, S. S. J Appl Polym Sci 1999, 72, 593.
8. Park, S. S.; Chae, S. H.; Im, S. S. J Polym Sci Part A: Polym Chem 1998, 36, 147.
9. Hoppens, N. C.; Hudnall, T. W.; Foster, A.; Booth, C. J. J Polym Sci Part A: Polym Chem 2004, 42, 3473.
10. Hayes, R. A. U.S. Pat. 6,485,819 (2002).
11. Fang, Q.; Hanna, M. A. Bioresour Technol 2001, 78, 115.
12. Witt, U.; Muller, R.-J.; Deckwer, W.-D. J Polym Environment 1995, 3, 215.
13. Seala, B. L.; Oterob, T. C.; Panitch, A., Materials Science and Engineering 34, 147, 2001.
14. Prowans, P.; Fray, M. E.; Slonecki, J. Biomaterials 2002, 23, 2973.
15. Renke-Gluszko, M.; Fray, M. E. Biomaterials 2004, 25, 5191.
16. Twarowska-Schmidt, K. Fibres Text Eastern Europe 2004, 12, 15.
17. Fumin, L.; Haile, W. A.; Tincher, M. E.; Harris, W. S. Eur. Pat. 1,330,350 (2003).
18. Wang, J. H.; Aimin, H. Wipo Pat. WO/2008/008068 (2008).
19. LU, F.; Ahaile, W.; Etincher, M.; Wiley, S. H. The World Intellectual Property Organization (WIPO), Switzerland, 2002.
20. Twarowska-Schmidt, K.; Ratajska, M. Fibres Text Eastern Eur 2005, 13, 71.
21. Clark, K. B.; Wheelwright, S. C. The Product Development Challenge: Competing through Speed, Quality, and Creativity; A Harvard Business Review Book: USA, 1995.
22. Tanguchi, G. Introduction to Quality Engineering; Asian Productivity Organization: Tokyo, 1986.
23. Zhang, Z. TQM Mag 1998, 10, 432.
24. Gardiner, W. P.; Gettinby, G. Experimental Design Techniques in Statistical Practice: A Practical Software-Based Approach; Horwood: England, 1998.
25. Capasso, V. Mathematical Modeling for Polymer Processing; Springer-Verlag: New York, 2003.
26. Vlachogiannis, J. G.; Roy, R. K. TOM Mag 2005, 17, 456.
27. Ellekjaer, M. R.; Bisgaard, S. Int J Quality Sci 1998, 3, 254.
28. Antony, J.; Perry, D.; Wang, C.; Kumar, M. Assembly Automation 2006, 26, 18.
29. Kijchavengkul, T.; Auras, R.; Rubino, M.; Ngouajio, M.; Fernandez, R. T. Chemosphere 2008, 71, 1607.
30. Saville, B. P. Physical Testing of Textiles; Woodhead: England, 1999.
31. Brody, H. Synthetic Fiber Materials; Longman Group UK Limited: London, 1994.
32. Stevens, E. S. Green Plastics, Plastics and the Environment; Princeton University Press: USA, 2001.
33. Warner, S. B. Fiber Science; Prentice-Hall: New Jersey, 1995.
34. Ziabicki, A. Fundamental of Fiber Formation; Wiley: London, 1976.
35. Hearle, J. W. S.; Miles, L. W. C. The Setting of Fibers and Fabrics; Marrow: England, 1971.
36. NICNAS, National Industrial Chemicals Notification and Assessment Scheme; CAS Number 60961–73-1: Australia 2003.
37. Connell, D. W. General Characteristics of Organic Compounds Which Exhibit Bioaccumulation, In Bioaccumulation of Xenobiotic Compounds; CRC Press: Boca Raton, USA, 1990.
38. Nabholz, J. V.; Miller, P.; Zeeman, M. Environmental Risk Assessment of the New Chemicals Under the Toxic Substances Control Act (TSCA) Section Five, Environmental Toxicology and Risk Assessment. ASTM STP 1179. Wayne G. Landis, Jane S. Hughes, and Michael, A.; Lewis ASTM: Philadelphia 1993.
39. Witt, U.; Einig, T.; Yamamoto, M.; Kleeberg, I.; Deckwer, W.-D.; Müller, R.-J. Chemosphere 2001, 44, 289.
40. Brydson, J. A. Flow Properties of Polymer Melts; George Godwin Limited: London, 1981.
41. Younes, B.; Fotheringham, A.; EL-Dessouky, H. M. Polym Eng Sci 2009, 49, 2492.
42. Younes, B.; Fotheringham, A.; EL-Dessouky, H. M. J Appl Polym Sci 2010, 118, 1270.
43. Younes, B.; Fotheringham, A. J Appl Polym Sci 2011, 119, 1896.
44. Younes, B.; Fotheringham, A.; EL-Dessouky, H. M.; Haddad, G. Int J Polym Mater 60, 316, 2011.
45. Walsh, P. The Yarn Book, How to Understand, Design and Use Yarn; A&C Black: London, 2006.
46. Giles, H. F.; Wagner, J. R.; Mount, E. M. Extrusion: the Definition Processing Guide and Hand Book; William Andrew Inc: Norwich, 2005.
47. Callister, W. Materials Science and Engineering: An Introduction; Wiley: New York, 1999.
48. Lochner, R. H.; Mater, J. E. Design for Quality; Chapman and Hall: London, 1990.
49. Phadke, M. S. Quality Engineering Using Robust Design; AT&T Bell Laboratories: USA, 1989.
50. Cawse, J. N. Experimental Design for Combinatorial and High Throughput Materials Development; Wiley: USA, 2003.
51. Montgomery, D. C. Design and Analysis of Experiment; Wiley: New York, 1997.
52. Meerveld, J. v.; Hutter, M.; Peters, G. W. M. J Non-Newtonian Fluid Mech 2008, 150, 177.
53. Ziabicki, A.; Jarecki, L.; Wasiak, A. Comput Theoret Polym Sci 1998, 8, 143.